

*Short Communication*

## **The Use of Phytic Acid Conversion Coating to Enhance the Corrosion Resistance of AZ91D Magnesium Alloy**

Qian Li, Peibo Liang\*, Yaqui Li, Zhipeng Ye, Bo Zhang, Chunyang Ji

Reliability and Environmental Engineering Research Center, China Electronic Product Reliability and Environmental Testing Research Institute, Guangzhou 510000, P R China

\*E-mail: [Peibo.Liang@163.com](mailto:Peibo.Liang@163.com)

*Received:* 8 February 2022 / *Accepted:* 10 March 2022 / *Published:* 7 August 2022

---

An environmentally friendly conversion coating based on phytic acid (PA) for AZ91D magnesium alloy was obtained by deposition. The influences of pH, time, PA concentration and temperature on corrosion resistance of PA conversion coating were discussed through orthogonal experiments, and the optimum processing parameters were confirmed. The results showed that pH is the most significant factor that influences the properties of PA conversion coating. Properties of PA conversion was investigated in details by electrochemical tests, scanning electron microscopy (SEM), Fourier transform infrared spectroscopy (FTIR) and X-ray photoelectron spectroscopy (XPS). The results indicated that the phytic acid conversion coating provided effective protection to the substrate of AZ91D alloy.

---

**Keywords:** Magnesium alloy; Chemical conversion coating; Phytic acid

### **1. INTRODUCTION**

Magnesium and its alloys are receiving more and more attention because of its excellent physical and mechanical properties[1-3]. Unfortunately, the applications of magnesium are restricted by its poor corrosion resistance under various service conditions for a long time[4-6]. To solve this problem, a number of surface treatment methods have been investigated to improve the corrosion resistance of magnesium alloys. Among them, conversion coatings are the most convenient and effective route in operative procedure[7-11]. Conversion coatings have been applied on substrates, with reported success, using different treatment methods including chromate, phosphate, permanganate, fluorozirconate, stannate and several other treatments[4, 12-14]. However, the use of chromate baths is being progressively restricted due to the high toxicity of the hexavalent chromium ions[1, 13, 15]. In recent years, some research has been carried out to search for more environment-friendly processes in surface modification of magnesium and its alloys[16-18].

Phytic acid ( $C_6H_6(H_2PO_4)_6$ , PA) is a natural and nontoxic organic macromolecule extracted from plant seeds, roots and stems[19-21]. A PA molecule consists of 24 oxygen atoms, 12 hydroxyl groups and 6 phosphate carboxyl groups. Due to the structure of active ligand oxygen atoms, PA can form stable chelates with many metal ions such as  $Zn^{2+}$ ,  $Fe^{2+}$ ,  $Fe^{3+}$ ,  $Ca^{2+}$  and  $Mg^{2+}$ , which may deposit on the metal substrates and block the corrosion reactions[3, 9, 22]. It has been reported that a PA conversion coating with anti-corrosion properties could be formed on the Mg alloy surface when immersed in a PA solution[18, 23-25]. Now that the chemical compositions and microstructures of magnesium alloys are different from each other, the reaction process of magnesium alloys with PA solution and its determinant roles are also different.

Towards a more comprehensive understanding of the PA conversion coating on magnesium and its alloys, we prepared a PA conversion coating a die-cast AZ91D magnesium alloy. Orthogonal experiments were used to analyze the processing parameters of the PA coating, XPS, FTIR spectrometer and SEM were used for compositional analysis and surface examinations of the coatings. The corrosion resistance of phytic acid conversion coating was estimated by the polarization curves.

## 2. EXPERIMENTAL DETAILS

### 2.1 Materials

A commercial die-cast AZ91D magnesium alloy was used in this study. Chemical composition of the AZ91D were listed in Table 1. The samples were cut into plates with dimensions of 25mm×25mm×2mm.

**Table 1.** Chemical composition of the die-cast AZ91D magnesium alloy

Elements	Al	Zn	Mn	Si	Fe	Ni	Mg
Comp/wt.%	9.03	0.65	0.20	0.024	<0.005	<0.002	Bal.

### 2.2 Preparation process of PA conversion coatings

The specimens were wet-ground to 2000# grit SiC paper, rinsed with distilled water, dried in a compressed hot air flow, and then pre-treated with 0.12 mol/L HCl solution to increase the activation of base alloy, the pickling time was 20 s. After the pre-treatment step, the samples were thoroughly washed using distilled water and dried for the following PA solution treatment step.

For designing the orthogonal experiments, the first step is to determine the main factors and the corresponding levels, PA concentration, pH value, treating temperature and treating time were selected as the four marked factors with three levels in the orthogonal-designed experiment, as shown in Table.2. Accordingly, a  $L_9(3^4)$  orthogonal array was obtained to guide the subsequent experiments as listed in Table 3, there are 9 experiments need to be carried in all. pH value of the PA solution was modified by triethylamine. All chemicals and reagents used were of analytical grade.

**Table 2.** Factors and levels of orthogonal experiment

Key Factors	Notations	Levels		
		1	2	3
PA solution concentration	A	5 g/L	7 g/L	10 g/L
PA solution pH value	B	6.5	7.5	8.5
Treating time	C	5 min	10 min	15 min
Treating temperature	D	25 °C	30 °C	40 °C

**Table 3.** Design of the L<sub>9</sub>(3<sup>4</sup>) orthogonal experiments

Experiment No.	A	B	C	D
1	1	1	1	1
2	1	2	2	2
3	1	3	3	3
4	2	1	2	3
5	2	2	3	1
6	2	3	1	2
7	3	1	3	2
8	3	2	1	3
9	3	3	2	1

### 2.3 Measurements

The surface and cross-sectional morphologies of the as-coated magnesium alloys were investigated by SEM (INSPECTF). XPS (ESCALAB250, Thermo VG Co.) was used to assess the chemical valence states of the elements in the conversion coating. The Al 2p, O 1s, Mg 1s, P 2p core level spectra and the core level spectra of all elements in alloy were monitored using monochromatic Al K $\alpha$  (1486.6 eV) radiation. The binding energy scale was calibrated to give a C1s line position at 284.5eV. Peak identification was performed with reference to an XPS data base. FTIR absorption spectra were measured to investigate the chemical nature of the organic conversion coating on the AZ91D surface. During FTIR measurement, a small portion of the PA conversion coating was scrapped off from the samples and ground to a fine power, mixed with KBr powder, and pressed into a pellet for the test.

The corrosion resistance of the conversion coating was monitored by potentiodynamic polarization tests using an PAR2273 Electrochemical Measurement System (EG&G). A three-electrode electrochemical cell was used with a Saturated Calomel Electrode (SCE) as the reference electrode and

a Platinum plate as the counter electrode. The as-coated magnesium alloy samples were employed as the working electrode, and were embedded in the mixture of paraffin and rosin (volume fraction of 1:1) leaving an exposed surface area of 1 cm<sup>2</sup>. 3.5 wt.% NaCl solution was used as the test electrolyte. A water bath was used to maintain the solutions at 25 ± 1°C during testing. Prior to potentiodynamic polarisation tests, the working electrode was immersed in the electrolyte until a stable corrosion potential was reached. Considering the corrosion behaviour of magnesium alloys, polarisation plots were drawn by single anodic curves and single cathodic curves at a scan rate of 0.33mV/s. The single polarisation tests were measured from stable open circuit potential to anodic direction or cathodic direction.

### 3. RESULTS AND DISCUSSION

#### 3.1 Orthogonal Experiment

As mentioned above, an  $L_9$  ( $3^4$ ) orthogonal array was used to analyze the effect of the combination of different processing parameters on the anti-corrosion properties of PA conversion coating on AZ91D alloy, and PA solution concentration, pH value, treating temperature and treating time are considered to the main four factors. Corrosion current density ( $i_{\text{corr}}$ ) was used as evaluation standard, which were got from the polarization plots of the samples in 3.5wt.% NaCl solution. Polarization curves of the 9 orthogonal experiments was shown in Fig.1, and the  $i_{\text{corr}}$  results corresponding to the orthogonal experiments are listed in Table 4.

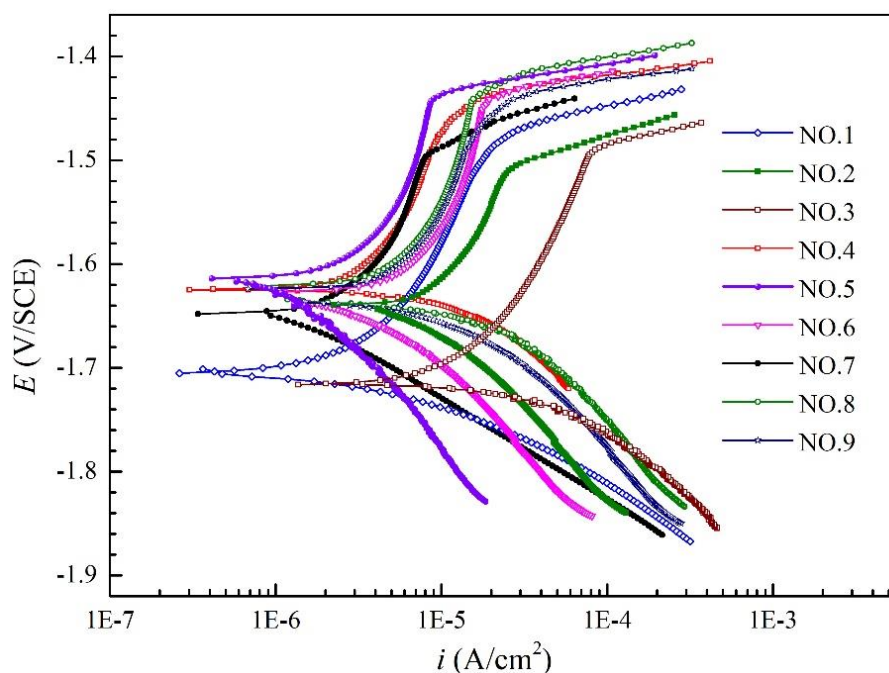


**Figure 1.** Polarization plots of AZ91D alloy with PA conversion coating prepared as during the orthogonal experiments in 3.5 wt.% NaCl solution

In Table 4, I, II, III presents the average value of  $i_{\text{corr}}$  for each factor under the three levels. For example, the factor A (pH value) at level 1 (pH=6.5), the mean value is calculated as  $(8.55+8.64+12.13)/3$ ,  $9.77 \mu\text{A}/\text{cm}^2$ . R is the range of the I, II, III values, which is the difference between maximum and minimum in I, II and III. According to the theory of orthogonal experiment, the R reflects the influence of each factor on the current density. From the results in Table 4, the effect of pH value on the range of  $i_{\text{corr}}$  was the maximum ( $3.43 \mu\text{A}/\text{cm}^2$ ), indicating that pH value was the most important factor, which influenced the quality of PA conversion coating the most. Concentration, treating time and treating temperature were the second, third and fourth important factor, and their effect on the range of  $i_{\text{corr}}$  were  $3.08 \mu\text{A}/\text{cm}^2$ ,  $2.47 \mu\text{A}/\text{cm}^2$ , and  $1.34 \mu\text{A}/\text{cm}^2$  respectively. Such results are consistent with some other works. Gao et al. investigated the formation and growth of a PA conversion coating on Mg-Li alloy [9], and also found that pH value effect the properties of PA coating most.

of the solution was the most important factor

In addition, the optimal combination of control factor levels can be determined by selecting the highest level for each control factor. From Table 4, the best corrosion resistance performance (the lowest  $i_{\text{corr}}$ ) was obtained by selecting the combination of control factors when the pH value was 7.5, treating time was 10 min, treating temperature was  $40 \text{ }^\circ\text{C}$ , PA concentration was 5 g/L.

**Table 4.** Results of the orthogonal experiment.

Experiment No.	A	B	C	D	$i_{\text{corr}} (\mu\text{A}/\text{cm}^2)$
1	1	1	1	1	8.55
2	1	2	2	2	8.64
3	1	3	3	3	12.13
4	2	1	2	3	7.48
5	2	2	3	1	3.14
6	2	3	1	2	8.40
7	3	1	3	2	6.24
8	3	2	1	3	8.58
9	3	3	2	1	7.25
I	$9.77 \mu\text{A}/\text{cm}^2$	$7.42 \mu\text{A}/\text{cm}^2$	$8.51 \mu\text{A}/\text{cm}^2$	$6.31 \mu\text{A}/\text{cm}^2$	
II	$6.34 \mu\text{A}/\text{cm}^2$	$6.79 \mu\text{A}/\text{cm}^2$	$7.79 \mu\text{A}/\text{cm}^2$	$7.76 \mu\text{A}/\text{cm}^2$	
III	$7.36 \mu\text{A}/\text{cm}^2$	$9.26 \mu\text{A}/\text{cm}^2$	$7.17 \mu\text{A}/\text{cm}^2$	$9.40 \mu\text{A}/\text{cm}^2$	
R	$3.43 \mu\text{A}/\text{cm}^2$	$2.47 \mu\text{A}/\text{cm}^2$	$1.34 \mu\text{A}/\text{cm}^2$	$3.08 \mu\text{A}/\text{cm}^2$	

Properties of the PA conversion coating formed under the optimal factors (pH=7.5, PA concentration 5 g/L,  $40 \text{ }^\circ\text{C}$ , 10min) was further evaluated by electrochemical test, SEM, XPS and FTIR.

### 3.2 SEM morphologies

SEM morphologies of the surface and cross section of the optimal PA conversion coating were shown in Fig.2. From the surface morphology in Fig.2 (a), two distinctive features, a reticular structure and smooth structure, can be found. The cross-sectional microstructure of the PA conversion coating in Fig.2 (b) indicates that a thin layer ( $0.5\ \mu\text{m} \sim 1\ \mu\text{m}$ ) adheres compactly to the substrate.

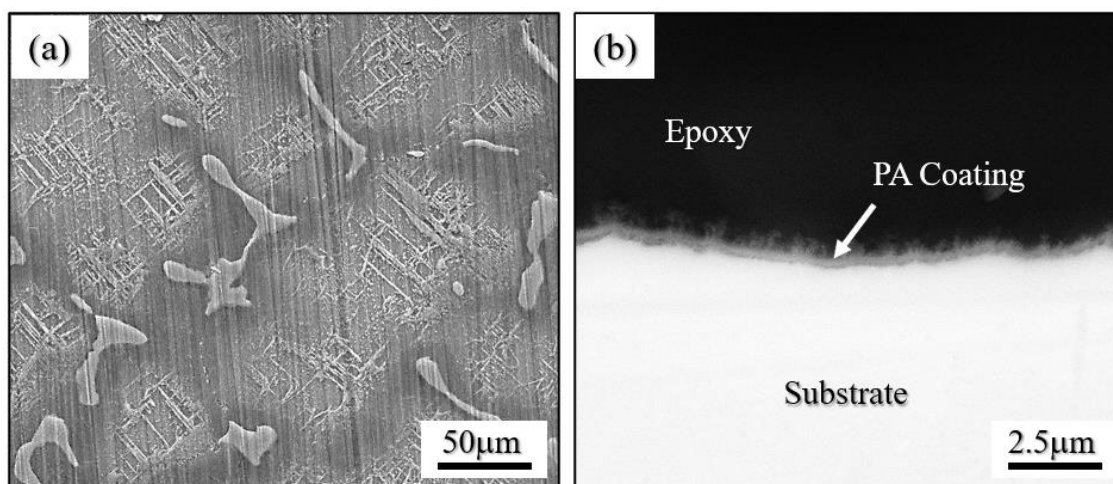


**Figure 2.** SEM morphologies of the optimal PA conversion coating (a): the surface morphology, (b) and cross-sectional morphology

### 3.3 Polarization plots

The polarization curves in Fig.3 showed that the electrochemical corrosion behavior of magnesium alloy with an optimal PA coating differed significantly from that of the uncoated alloy. Firstly, the anodic branch of the coated sample disappears a passivation behavior, and the anodic current density appears to maintain a steady state with changes in potential in the region between  $-1.6\ \text{V/SCE} \sim -1.4\ \text{V/SCE}$ , which indicates the formation of a more stable and resistant corrosion product layer compared to the bare magnesium alloy, and changes the anodic process of the AZ91D alloy. In addition, the cathodic current density of the coated sample is also lower than that of the bare AZ91D alloy, implying that the cathodic reactions were also inhibited by the PA conversion coating. Since the anodic and cathodic process were both restricted, the corrosion current density of the Mg alloys with the optimal PA conversion coating is obviously lower than that of the substrate at any given potential from Fig.3, thus confirming that PA conversion coating provides effective protection for the magnesium alloy.

Magnesium alloys are usually oxidized in air forming an unstable and non-protective oxide film on the surface. The results however reveal that the formation of magnesium phosphate and metaphosphate on the coating provides better protection for the magnesium alloy.

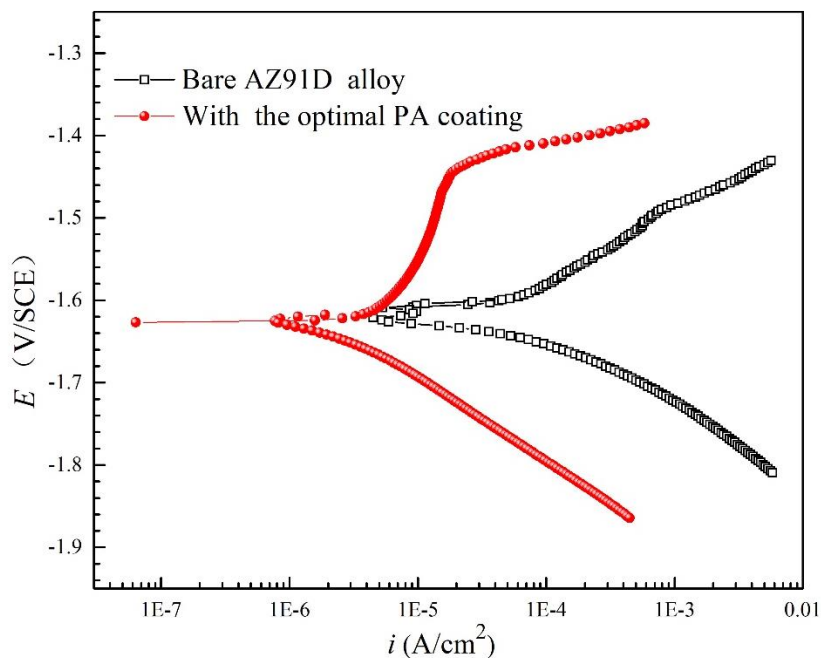


**Figure 3.** Potentiodynamic polarization curves of AZ91D alloy with and without a PA coating in 3.5 wt.% NaCl solution

From the orthogonal experiment, it is proved that pH value of the PA solution is the most important factor than influences the corrosion resistance of the conversion coating on Mg alloy, thus, we further investigated the properties of PA conversion coating under different pH values in detail. The surface morphologies of PA conversion coating formed in different pH treatment solutions have been shown in Fig.4. The pH value was 6.5, 7.5 and 8.5, while treating time was 10 min, treating temperature was 40 °C, PA concentration was 5 g/L. When the pH of treatment solution is 6.5, there are few ramiform and reticular structures on the coating. However, at neutral and alkaline treatment solution (pH =7.5 and pH = 8.5), the ramiform and reticular structures were obvious.

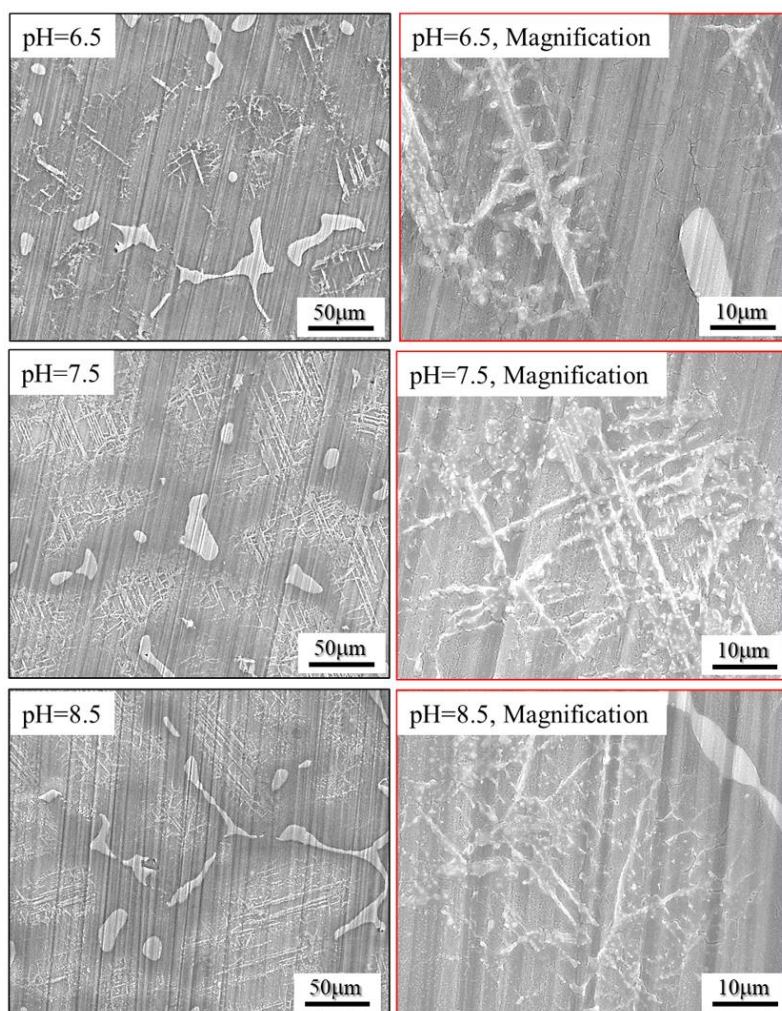


**Figure 4.** The surface morphologies of PA conversion coating formed in different pH treatment solutions

### 3.4 XPS results

To understand the compositions and chemical state of the elements in the conversion coatings, XPS was used to analyze the PA conversion coatings and the result is shown in Fig.5. It was revealed that that O, Mg, C, P and Al elements are in the coatings.

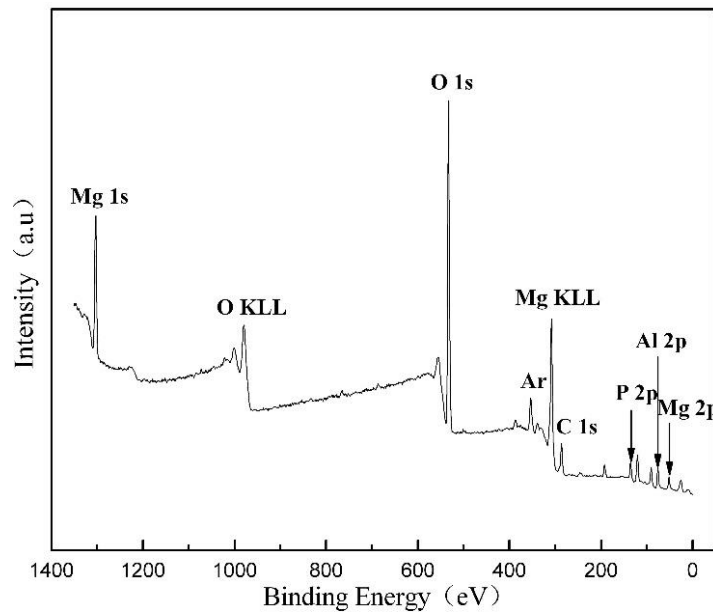


**Figure 5.** XPS spectra of the optimal PA conversion coating on AZ91D magnesium alloy

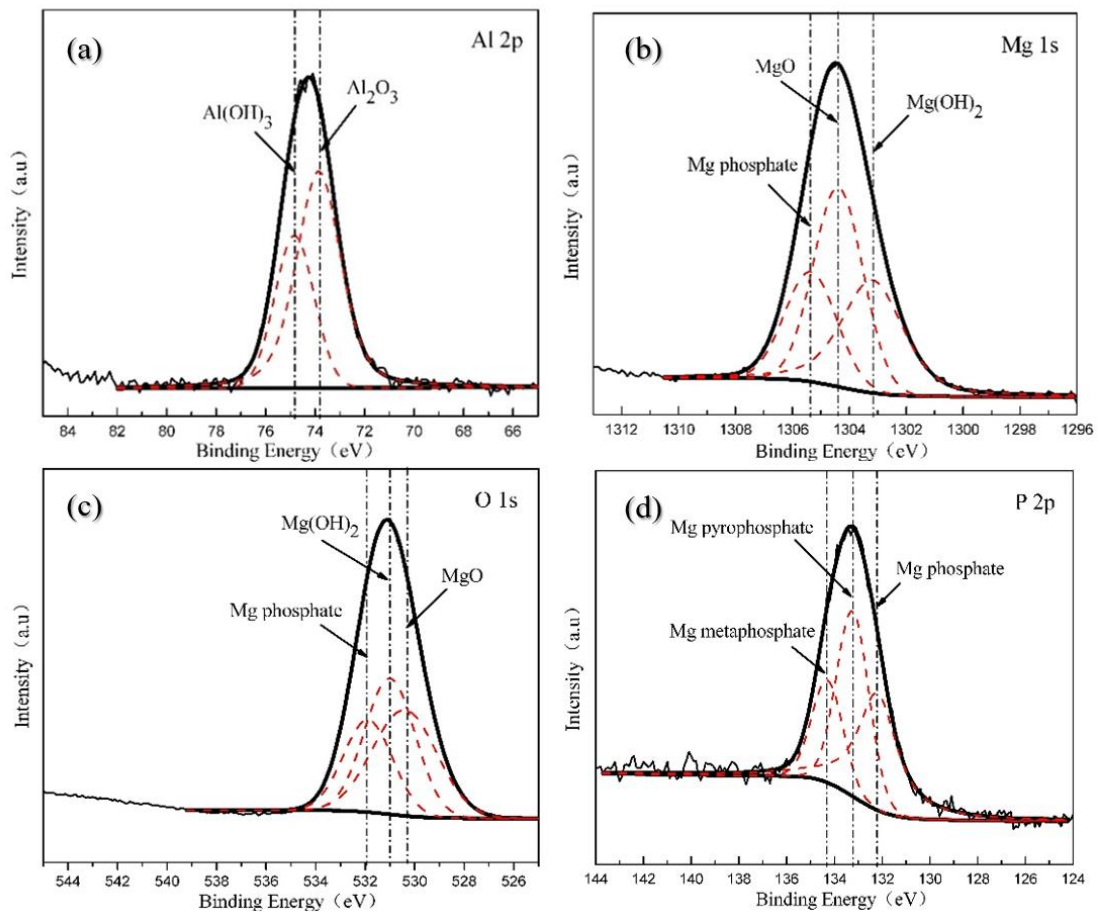


**Figure 6.** High resolution spectra of the elements in the PA conversion coating (a) Al 2p; (b) Mg 1s; (c) O 1s; (d) P 2p

Fig. 6 further shows the high-resolution spectra of the major alloy elements in the PA conversion coatings. The peaks of Al 2p (Fig.6 (a)) at 73.9 eV and 74.9 eV are attributed to  $\text{Al}_2\text{O}_3$  and  $\text{Al}(\text{OH})_3$  respectively. Fig.6 (b) shows that the XPS spectrum of Mg 1s is decomposed into three peaks at 1303.2 eV, 1304.4 eV and 1305.3 eV corresponding to  $\text{Mg}(\text{OH})_2$ , MgO and  $\text{Mg}_3(\text{PO}_4)_2$  respectively. Fig.6 (c) shows that the three O 1s peaks at 530.4 eV (assigned to metal oxides), at 531.0 eV (assigned to hydroxides) and at 532.0 eV (assigned to phosphates) appeared in the conversion coating on magnesium alloy. The typical P 2p peak is shown in Fig.6 (d). The peaks of P 2p at 132.2 eV, 133.2 eV and 134.3 eV are attributed to magnesium phosphate, magnesium pyrophosphate and magnesium metaphosphate respectively [27, 28]. From the results of the XPS, it can be inferred that  $\text{Mg}(\text{OH})_2$ , MgO,  $\text{Mg}_3(\text{PO}_4)_2$  Mg metaphosphate and Mg pyrophosphate predominate in the conversion coating, and that  $\text{Al}(\text{OH})_3$  and  $\text{Al}_2\text{O}_3$  are also present in the coating.

### 3.5 FTIR results

In order to validate the above analysis, the FTIR spectra of PA conversion coatings on AZ91D and phytic acid are shown in Fig. 7. Absorption peaks for hydroxyl were observed at  $3413\text{ cm}^{-1}$  and  $1644\text{ cm}^{-1}$  in PA. The absorption peak at  $2356\text{ cm}^{-1}$  and  $870\text{ cm}^{-1}$  is assigned as P-OH,  $1130\text{ cm}^{-1}$  as P=O and  $1010\text{ cm}^{-1}$  as P-O-C. For the PA conversion coating, the adsorption peak at  $2356\text{ cm}^{-1}$  and  $870\text{ cm}^{-1}$  have disappeared and new peaks form at  $1030\text{ cm}^{-1} \sim 967\text{ cm}^{-1}$  in PA conversion coating, which suggests that P-OH group reacts with magnesium alloy and new products form in the coating [29,30]. The existence of peaks of O-H  $\sim 3387\text{ cm}^{-1}$  and H-OH  $\sim 1640\text{ cm}^{-1}$  indicates that hydroxyl still exists in PA coating.

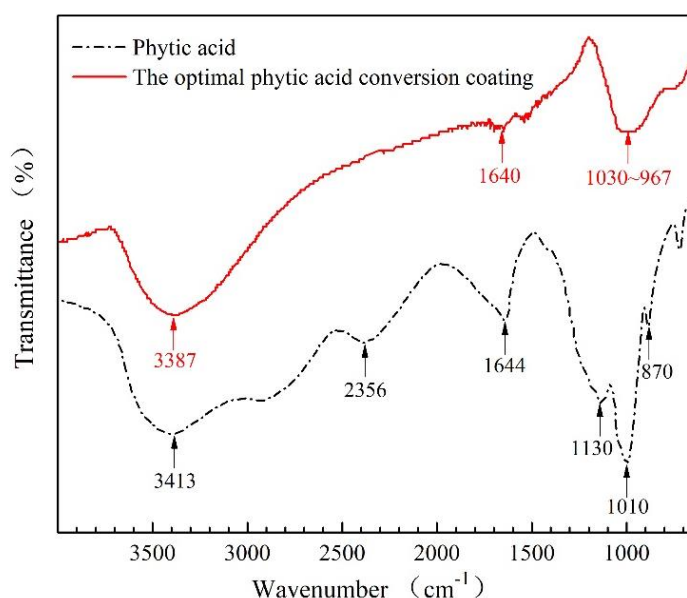


**Figure 7.** Infrared spectrum of PA and the PA conversion coatings on AZ91D

#### 4. CONCLUSION

In this work, an anticorrosive PA conversion coating for AZ91D magnesium alloy has been developed.

(1) The optimal processing parameters for the anticorrosion property of the PA coating were confirmed as follows: pH value was 7.5, PA concentration was 5 g/L, treating temperature was 40 °C and treating time was 10min.

(2) The pH value of the solution was the main factor influencing the anticorrosion property of the PA conversion coating on AZ91D.

(3) Chelate compounds were formed between PA and  $Mg^{2+}$  or  $Al^{3+}$  during the formation of PA conversion coating.

#### DECLARATION OF COMPETING INTEREST

The authors declare that they have no known competing financial interests or personal relationships that could have appeared to influence the work reported in this paper.

#### ACKNOWLEDGEMENTS

This work is supported by the National Key Research and Development Program of China (No. 2018YFB2003600).

#### References

1. J. Qi, Z. Ye, N. Gong, X. Qu, D. Mercier, J. Światowska, P. Skeldon, P. Marcus, *Corrosion Science*, 186 (2021) 109459.
2. Q. Wu, B.X. Yu, P. Zhou, T. Zhang, F.H. Wang, *Materials Chemistry and Physics*, 273 (2021) 125121.
3. S.K. Yang, R.X. Sun, K.Z. Chen, *Chemical Engineering Journal*, 428 (2022) 131198.
4. P. Zhou, B.X. Yu, Y.J. Hou, G.Q. Duan, L.X. Yang, B. Zhang, T. Zhang, F.H. Wang, *Corrosion Science*, 178 (2021) 109069.
5. Y. Zhou, P. Zhang, L.H.Z. Su, B.M. Fan, F.A. Yang, *Materials Letters*, 304 (2021) 130640.
6. Y. Zhou, P. Zhang, F.A. Yan, *Materials Letters*, 284 (2021) 128930.
7. S. Chen, S. Zhao, M.Y. Chen, X. Zhang, J. Zhang, X. Li, H. Zhang, X.H. Shen, J. Wang, N. Huang, *Applied Surface Science*, 463 (2019) 953.
8. X.F. Cui, Q.F. Li, Y. Li, F.H. Wang, G. Jin, M.H. Ding, *Applied Surface Science*, 255 (2008) 2098.
9. L.L. Gao, C.H. Zhang, M.L. Zhang, X.M. Huang, X. Jiang, *Journal of Alloys and Compounds*, 485 (2009) 789.
10. L.B. Boinovich, E.B. Modin, A.R. Sayfutdinova, *et al. ACS Nano*, 11 (2017) 10113.
11. F.T. Cao, J. Wei, J.H. Dong, W. Ke, *Corrosion Science*, 100 (2015) 365.
12. S.Y. Jian, C.Y. Yang, J.K. Chang, *Applied Surface Science*, 510 (2020) 145385.
13. C.Y. Zhang, S.Y. Zhang, D.W. Sun, J.J. Lin, F.C. Meng, H.N. Liu, *Journal of Magnesium and Alloys*, 9 (2021) 1246.
14. S.V.S. Prasad, S.B. Prasad, K. Verma, R.K. Mishra, V. Kumar, S. Singh, *Journal of Magnesium and Alloys*, 10 (2022) 1.
15. W. Zai, X.R. Zhang, Y.C. Su, H.C. Man, G.Y. Li, J.S. Lian, *Surface and Coatings Technology*, 397 (2020) 125919.

16. S. Jiang, S. Cai, F.Y. Zhang, P. Xu, R. Ling, Y. Li, Y.Y. Jiang, G.H. Xu, *Materials Science and Engineering: C*, 91 (2018) 218.
17. J.R. Liu, Y.N. Guo, W.D. Huang, *Surface and Coatings Technology*, 201 (2006) 1536.
18. M. Yeganeh, N. Mohammadi. *Journal of Magnesium and Alloys*, 6 (2018) 59.
19. L. Liu, Q.Y. Yang, L. Huang, X.M. Liu, Y.Q. Liang, Z.D. Cui, X.J. Yang, S.L. Zhu, Z.Y. Li, Y.F. Zheng, K.W.K. Yeung, S.L. Wu, *Applied Surface Science*, 484 (2019) 511.
20. J.F. Ou, X. Chen, *Journal of Alloys and Compounds*, 787 (2019) 145.
21. F.S. Pan, X. Yang, D.F. Zhang, *Applied Surface Science*, 255 (2009) 8363.
22. J.E. Gray, B. Luan, *Journal of Alloys and Compounds*, 336 (2002) 88.
23. S.J. Liao, B.X. Yu, B. Zhang, P. Zhou, T. Zhang, F.H. Wang, *Corrosion Science*, 191 (2021) 109725.
24. S.J. Liao, B.X. Yu, X.L. Zhang, X. Lu, P. Zhou, C.Y. Zhang, X.B. Chen, T. Zhang, F.H. Wang, *Journal of Magnesium and Alloys*, 9 (2021) 505.
25. Y. Liu, Y. Zhang, Y.L. Wang, Y.Q. Tian, L.S. Chen, *Journal of Alloys and Compounds*, 865 (2021) 161001.
26. Z.Z. Yin, W. Huang, X. Song, Q. Zhang, R.C. Zeng, *Frontiers of Materials Science*, 14 (2020) 296.
27. R.Y. Zhang, S. Cai, G.H. Xu, H. Zhao, Y. Li, X.X. Wang, K. Huang, M.G. Ren, X.D. Wu, *Applied Surface Science*, 313 (2014) 896.
28. H.F. Gao, H.Q. Tan, J. Li, Y.Q. Wang, J.Q. Xun, *Surface and Coatings Technology*, 212 (2012) 32.
29. X.F. Cui, Y. Li, Q.F. Li, G. Jin, M.H. Ding, F.H. Wang, *Materials Chemistry and Physics*, 111 (2008) 503.
30. M.L. Zhang, R.R. Chen, X.M. Liu, Q. Liu, J.Y. Liu, J. Yu, P.L. Liu, L.T. Gao, J. Wang, *Journal of Alloys and Compounds*, 818 (2020) 152875

© 2022 The Authors. Published by ESG ([www.electrochemsci.org](http://www.electrochemsci.org)). This article is an open access article distributed under the terms and conditions of the Creative Commons Attribution license (<http://creativecommons.org/licenses/by/4.0/>).